Electronic Supplementary Material (ESI) for Nanoscale
This journal is © The Royal Society of Chemistry 2013

Supporting Information for

Nanoparticle Dispersion in Polymer Nanocomposites by Spin-Diffusion-Averaged Paramagnetic Enhanced NMR Relaxometry

Bo Xu,[a]* Johannes E. Leisen,[b] and Haskell W. Beckham[a]

[a]*School of Materials Science and Engineering, Georgia Institute of Technology, 801 Ferst Drive, Atlanta, GA 30332 USA.*
[b]*School of Chemistry and Biochemistry, Georgia Institute of Technology, 901 Atlantic Drive, Atlanta, GA 30332 USA.*

*E-mail: (B. X.) bxu6@gatech.edu

This file contains:

Section 1. Experimental Details

A. Materials

The materials chosen for this work are polypropylene-montmorillonite (PP-MMT) nanocomposites. The details on these materials have been reported previously.[1] Isotactic PP (Total Petrochemicals) and organically modified MMT, Cloisite 15A (Southern Clay) and 3 wt% PP-*g*-maleic anhydride (PP-MA) (Dupont), and a pure PP/PP-MA blend were prepared using melt compounding. In the text, the PP/PP-MA blend and the nanocomposite are simply referred to as 'PP' and 'PP-MMT', respectively. The PP-MMT-2.7 denotes a nanocomposite containing 2.7 wt% of the actual MMT content. The PP and PP-MMT were compression-molded at 190 °C to form sheets with a thickness of 1 mm. This was followed by equi-biaxial stretching in a home-built apparatus for both PP and

Electronic Supplementary Material (ESI) for Nanoscale
This journal is © The Royal Society of Chemistry 2013

nanocomposite sheets. A series of PP and PP-MMT-2.7 films with stretch ratios (λ = final length/initial length) of 1.5 to 3.5 were prepared by stretching at 150 °C with a strain rate of 16 s^{-1}. The unstretched samples with λ = 1 are the compression-molded sheets.

B. Methods

The details of NMR and TEM measurements were reported previously.[1] Briefly, ^{1}H saturation-recovery NMR experiments were performed at room temperature using a two-channel 7-mm magic-angle spinning (MAS) probe in a Bruker DSX-300 solid-state NMR spectrometer (300 MHz, 7.05 T). Although an MAS probe was employed, all relaxation measurements were made without sample spinning.

High resolution TEM images (Phillips CM100) were recorded on ultra-thin samples (typically 60 nm). For each sample a total of 5 – 7 representative images were analyzed manually using the software package ImageJ version 1.24o (NIH). The interparticle spacing (IPS) and its distribution were determined through a method modified from the free-path spacing measurement (FPSM), which has been reported by Luo and Koo.[2, 3] For the unstretched sample, the number of measurements (sampling number), N is 772; for the stretched sample, $N > 450$. A stack of clay platelets was taken as a single particle. This process is different from that of the FPSM. We made this modification for the following reasons: the number of platelets within a stack is hardly discernible by the naked eye in the TEM images, and our model focuses on describing the relaxation of polymer domains between particles rather than that of protons inside stacks. Furthermore, distances less than 5 nm between nearby particles were not counted; such structures are considered intercalated stacks. The relaxation of nuclei in such a stack is governed by the relaxation of surface nuclei rather than by the spin diffusion process described in our model.

Following the FPSM protocol, two perpendicular arrays of parallel lines were placed over the TEM images of the unstretched sample (the isotropic sample), so that the measurements could be conducted in orthogonal directions. For the stretched samples, the array of parallel lines was applied along the direction normal to the primary direction of particle alignment. Note that these placed lines only served as a guide for our measurements. For example, if particles appeared in the lattices or between lines rather than intersect the lines, these particles were also included in the measurements. Through this exercise, face-to-face distances, or interparticle spacings, were measured.

Electronic Supplementary Material (ESI) for Nanoscale
This journal is © The Royal Society of Chemistry 2013

Section 2. Demonstration of TEM Image Analysis

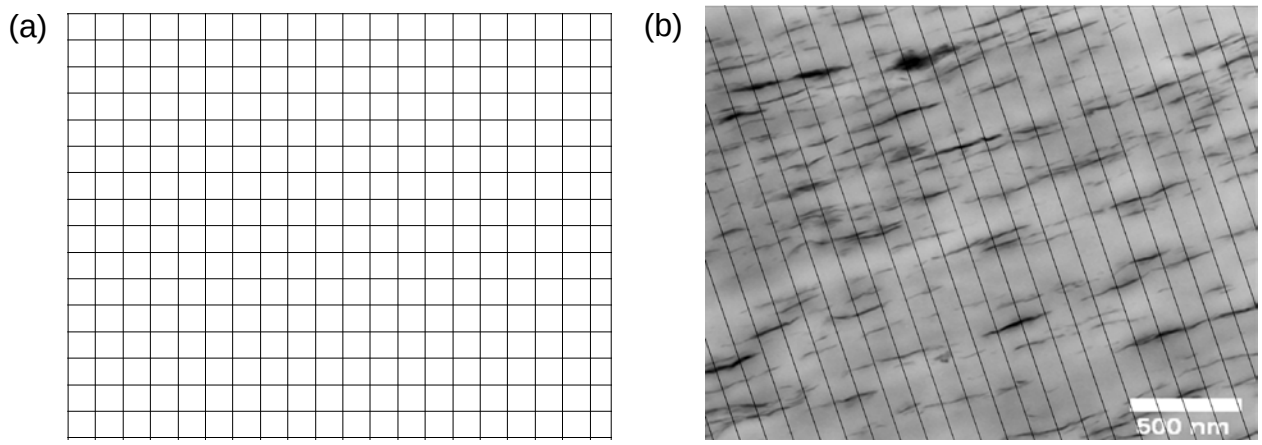

Figure S1. Two examples of TEM images onto which arrays of parallel lines were placed for measurements of interparticle spacings: (a) two perpendicular arrays for the unstretched sample; (b) an array of parallel lines was applied along the direction normal to the primary direction of particle alignment. Note that these arrays of lines only served as guides for the measurements.

Section 3. Model Development: Magnetization Growth in Polymer/Clay Nanocomposites

As discussed in the main text, the time-dependent magnetization growth of surface nuclei can be described as

$$m_s(t) = m_0(1 - e^{-t/T_{1,s}}) \tag{S1}$$

where m_0 is the equilibrium magnetization per spin.

The mathematical description of T_1 relaxation in our model requires a solution of the well-known Torrey-Bloch equation governing the evolution of the longitudinal component of nuclear magnetization,[4] which is expressed in one dimension as

$$\frac{\partial m(x,t)}{\partial t} = D\frac{\partial^2 m(x,t)}{\partial x^2} - \frac{1}{T_{1,m}}[m(x,t) - m_o] \tag{S2}$$

where D is the bulk spin diffusion coefficient (uniform, not a function of x), $1/T_{1,m}$ is the bulk spin relaxation rate, and m is the magnetization per spin. A general solution to Eq. S2 is

$$m(x,t) = m_0 - \psi(x,t)e^{-t/T_{1,m}} \tag{S3}$$

where $\psi(x, t)$ fulfills the standard diffusion equation given by

Electronic Supplementary Material (ESI) for Nanoscale
This journal is © The Royal Society of Chemistry 2013

$$\frac{\partial \psi(x,t)}{\partial t} = D\frac{\partial^2 \psi(x,t)}{\partial x^2} \tag{S4}$$

The initial and boundary conditions for the saturation-recovery experiment are as follows:

$$\psi = m_0 \text{ for } -L < x < +L \text{ at } t = 0 \tag{S5}$$

$$\psi = m_0 \, e^{-\beta t} \text{ at } x = \pm L \text{ for } t > 0. \tag{S6}$$

where

$$\beta = \frac{1}{T_{1,s}} - \frac{1}{T_{1,m}} \tag{S7}$$

Here, β is the difference between relaxation rates of the surface and bulk nuclei. Under these conditions, an analytical solution to Eq. S2 is obtained as the known solution of the diffusion equation for time-dependent surface concentration given by Carslaw and Jaeger.[5] The detected signal is $M(t) = \int m\,(x, t)\, d\Omega$ (M_0 is the total equilibrium magnetization). Thus, as the normalized magnetization in the domain of interest, the detected NMR signal can be obtained as follows:

$$\frac{M(t)}{M_o} = 1 - \left(\frac{4D}{\beta\Delta^2}\right)^{1/2} \tan\left(\frac{\beta\Delta^2}{4D}\right)^{1/2} \exp(-t/T_{1,s}) - \frac{8}{\pi^2}\sum_{n=0}^{\infty}\frac{1}{(2n+1)^2}\left[\frac{1}{1-(2n+1)^2\pi^2 D/(\beta\Delta^2)}\right]\exp\left[-\left(\frac{(2n+1)^2\pi^2 D}{\Delta^2} + \frac{1}{T_{1,m}}\right)t\right] \tag{1}$$

where $\Delta \approx 2L$ at $L >> b$ (see main text for more details).

For a theoretical analysis of our model, considering the IPS distribution in polymer-clay nanocomposites, we incorporated a distribution function into Eq. 1. For a continuous IPS distribution, the magnetization profile averaged over the upper and lower limits (Δ_{max}) and (Δ_{min}) is given by

$$\left\langle \frac{M(t)}{M_0} \right\rangle = \int_{\Delta_{min}}^{\Delta_{max}} P(\Delta)\frac{M(t)}{M_0}\, d\Delta \tag{S8}$$

where $\int_{\Delta min}^{\Delta max} P(\Delta) d\Delta = 1$. Through choice of integration limits, we ensure that Δ remains within a physical limit of $\Delta >> 2b$. Despite no *a priori* knowledge about the IPS distribution, it is reasonable to assume a Gaussian distribution for the interparticle spacing

$$P(\Delta) = \frac{1}{\sigma\sqrt{2\pi}} e^{-\frac{1}{2}\left(\frac{\Delta - \langle\Delta\rangle}{\sigma}\right)^2} \tag{S9}$$

where $\langle\Delta\rangle$ is the average IPS, and σ is the standard deviation and a measure of the homogeneity of the particle distribution. Note that the distribution of interparticle spacings measured from TEM

Electronic Supplementary Material (ESI) for Nanoscale
This journal is © The Royal Society of Chemistry 2013

images has been fitted by several functions including the log-normal distribution,[2] and the Gaussian distribution.[3]

Section 4. Model Analysis

A. Relaxation of Surface Nuclei

We applied Eqs. 1, S8 and S9 to describe the magnetization growth for a system with D = 0.7 nm^2/ms, $T_{1,m}$ = 1.635 s, and $\langle\Delta\rangle$ = 50 nm. The magnetization growth profiles are shown in Fig. S2a for a broad range of surface relaxation times, $T_{1,s}$. The same data were plotted as $\ln(1 - \langle M(t)/M_o\rangle)$ versus recovery time, t, from which the $T_{1,PCN}$ values were determined from the slopes. Fig. S2b shows the resulting $T_{1,PCN}$ values as a function of $T_{1,s}$.

The overall relaxation is significantly delayed upon lowering the relaxation efficiency of surface nuclei (i.e., longer $T_{1,s}$ values), especially for $T_{1,s}$ > 10 ms (cf. Fig. S2a). For sufficiently efficient surface relaxation (i.e., characterized by $T_{1,s} \leq$ 10 ms), the $T_{1,PCN}$ is nearly the same (cf. Fig. S2b).

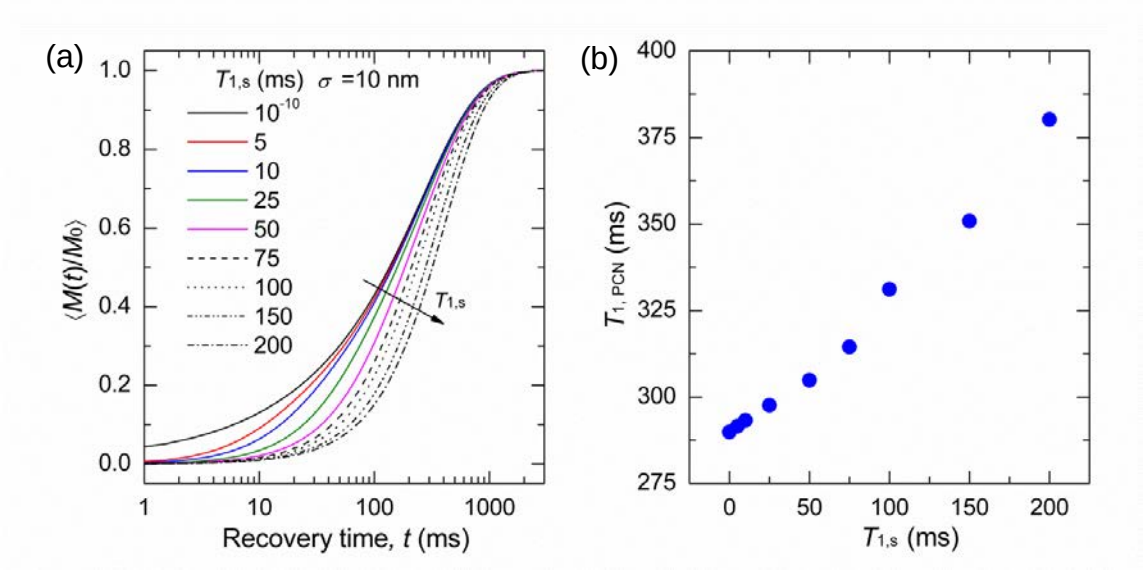

Figure S2. (a) Normalized magnetization versus recovery time calculated using Eqs. 1, S8 and S9 for D = 0.7 nm^2/ms, $T_{1,m}$ = 1.635 s, $\langle\Delta\rangle$ = 50 nm, Δ_{max} = 100 nm, Δ_{min} = 5 nm, σ = 10 nm and different $T_{1,s}$ values. The arrow indicates increasing $T_{1,s}$. The overall relaxation is significantly delayed upon lowering the relaxation efficiency of surface nuclei (i.e., longer $T_{1,s}$ values), especially for $T_{1,s}$ > 10 ms. (b) Relaxation times ($T_{1,PCN}$) calculated from a linear fit of $\ln(1 - \langle M(t)/M_0\rangle)$ versus time t, plotted from the same data shown in (a). For sufficiently efficient surface relaxation (i.e., characterized by $T_{1,s} \leq$ 10 ms), the $T_{1,PCN}$ is nearly the same.

Electronic Supplementary Material (ESI) for Nanoscale
This journal is © The Royal Society of Chemistry 2013

B. Clay Distribution Homogeneity

The magnetization growth curves were calculated for materials with $T_{1,s}$ = 5 ms, D = 0.7 nm^2/ms, $T_{1,m}$ = 1.635 s, $\langle\Delta\rangle$ = 50 nm, and standard deviations (σ) of 0.5, 5, 10 and 15 nm (cf. Fig. S3). For larger σ (i.e., lower homogeneity), magnetization recovery is faster at short times but slower at long times.

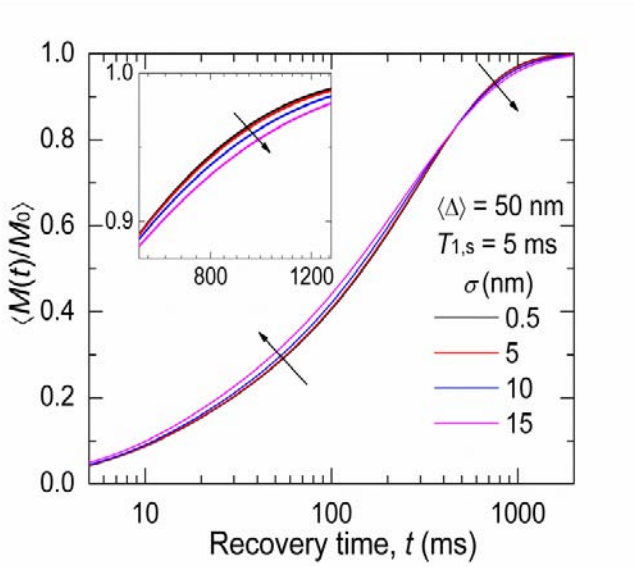

Figure S3. Normalized magnetization, $\langle M(t)/M_o\rangle$, versus recovery time, t, calculated using Eqs. 1, S8 and S9 for $T_{1,s}$ = 5 ms, D = 0.7 nm^2/ms, $T_{1,m}$ = 1.635 s, $\langle\Delta\rangle$ = 50 nm, Δ_{max} = 100 nm, Δ_{min} = 5 nm, and standard deviations (σ) of 0.5, 5, 10 and 15 nm. The inset shows the profiles at t = 600 – 1300 ms. The arrows indicate increasing σ. For larger σ (i.e., lower homogeneity), magnetization recovery is faster at short times but slower at long times.

Section 5. Fitting Parameters

A. Determination of Spin Diffusion Coefficient, *D*

In our polypropylene samples, the average size of the polymer matrix between clay particles is much larger than 10 nm and constitutes both amorphous and crystalline domains. Thus, an average effective spin diffusion coefficient was calculated:[7-9]

$$\sqrt{D_{s,eff}} = \frac{\sqrt{D_a D_c}}{(\sqrt{D_a} + \sqrt{D_c})/2} \qquad \text{(S10)}$$

where D_a and D_c are the spin-diffusion coefficients of amorphous and crystalline phases, respectively. The spin diffusion coefficients of $D_a \approx 0.13$ nm^2/ms and $D_c \approx 0.62$ nm^2/ms in isotactic PP at room temperature have been determined through static linewidths by Hedesiu et al.[6] Using these values, $D_{s,eff}$ = 0.24 nm^2/ms was calculated. Following the same approach described by

Electronic Supplementary Material (ESI) for Nanoscale
This journal is © The Royal Society of Chemistry 2013

Hedesiu et al., we estimated the spin-diffusion coefficient for the nanocomposites and found the same value of $D = 0.24 \pm 0.05$ nm^2/ms. Note that the value of D used here is meant to characterize spin diffusion along the polymer backbone, between different polymer chains, and even among multiple phases. Thus, the D values employed in our model should be similar to those measured by Meurer et al.,[10] rather than those obtained by more localized measurement techniques.[11-13] Meurer et al. claimed that their D values reflected spin diffusion by flips flops between nuclear spins belonging to different chains or even different phases.[10]

B. Estimation of Relaxation Time of Surface Nuclei, $T_{1,s}$

At 300 MHz, the measured T_1 of the observable ^{1}Hs in Cloisite 15A is 10 ms.[1] The distance between the observable ^{1}Hs and the paramagnetic Fe^{3+} ions is $r = 0.5 – 1.6$ nm, with the lower boundary being half the platelet thickness and upper boundary calculated as half the basal spacing, 3.2 nm, divided by 2. Using $T_{1,s} = 10$ ms and $1/T_{1,s} \propto r^{-6}$,[14-17] we estimated the average relaxation time to be $T_{1,s} = 3$ ms for the surface nuclei in a 0.4-nm-thick layer around the clay particles.

Section 6. Table S1

Table S1. Comparison of Interparticle Spacings (Δ) from NMR and TEM for PP-MMT Films

stretch ratio, λ	1	1.5	2	2.5	3	3.5
Δ_{TEM_ave} (nm) [a]	215 ± 137	167 ± 111	131 ± 92	111 ± 89	105 ± 71	96 ± 64
Δ_{TEM_rms} (nm) [a]	254 ± 298	210 ± 227	171 ± 186	131 ± 147	123 ± 141	115 ± 142
Δ_{NMR} (nm) [b]	211± 22	232 ± 26	180 ± 15	138 ± 11	134 ± 10	122 ± 9

[a]Measured using a modified method reported by Luo and Koo:[2, 3] Δ_{TEM_ave} is the arithmetic average interparticle spacing (IPS); Δ_{TEM_rms} is the root-mean-square or quadratic mean IPS. [b]Calculated by fitting the NMR relaxation curves to Eq. 1; the resulting relaxation time of the surface nuclei, $T_{1,s}$, was ~ 5 ms (± 2 ms) for all nanocomposite samples.

References

1 B. Xu, J. Leisen, H. W. Beckham, R. Abu-Zurayk, E. Harkin-Jones, T. McNally, *Macromolecules* 2009, **42**, 8959-8968.
2 Z. P. Luo, J. H. Koo, *Polymer* 2008 **49**, 1841-1852.
3 Z. P. Luo, J. H. Koo, *J. Microscopy* 2007, **225**, 118-125.
4 H. C. Torrey, 563 (1956). *Phys. Rev. B* 1956, **104**, 563-565.
5 H. S. Carslaw, J. C. Jaeger, *Conduction of Heat in Solids*, 2nd ed., Clarendon Press, Oxford, **1986**.
6 C. Hedesiu, D. E. Demco, R. Kleppinger, G. Vanden Poel, W. Gijsbers, B. Blumich, K. Remerie, V. M. Litvinov, *Macromolecules* 2007, **40**, 3977-3989.
7 K. Schmidt-Rohr, J. Clauss, H. W. Spiess, *Macromolecules* 1992, **25**, 3273-3277.
8 F. Mellinger, M. Wilhelm, H. W. Spiess, *Macromolecules* 1999, **32**, 4686-4691.

9 K. Schmidt-Rohr, H. W. Spiess, *Multidimensional Solid-State NMR and Polymers*, Academic Press, London, **1994**.
10 B. Meurer, G. Weill, *Macromolecular Chemistry and Physics* 2008, **209**, 212-219.
11 X. W. Wang, J. L. White, *Macromolecules* 2002, **35**, 3795-3798.
12 X. Jia, J. Wolak, X. W. Wang, J. L. White, *Macromolecules* 2003, **36**, 712-718.
13 Q. Chen, K. Schmidt-Rohr, *Solid State Nucl. Magn. Reson.* 2006, **29**, 142-152.
14 N. Bloembergen, *Physica* 1949, **15**, 386-426.
15 P. G. de Gennes, *J. Phys. Chem. Solids* 1958, **7**, 345-350.
16 A. Abragam, *The Principles of Nuclear Magnetism*, Clarendon Press, Oxford, **1961**.
17 W. E. Blumberg, *Phys. Rev.* 1960, **119**, 79-84.